

COMPTON SCATTERING FROM HYDROGEN BETWEEN 5 AND 17 GEV*

R. L. Anderson, D. Gustavson, J. Johnson,
I. Overman, D. Ritson and B. H. Wiik
Stanford Linear Accelerator Center
Stanford University, Stanford, California 94305

R. Talman
Cornell University
Ithaca, New York 14850

J. K. Walker
National Accelerator Laboratory
Batavia, Illinois 60510

D. Worcester
Harvard University
Cambridge, Massachusetts 02138

ABSTRACT

Measurements have been made on Compton scattering at the Stanford Linear Accelerator Center for photon energies between 5 and 17 GeV and t -values from -0.06 to -1.1 $(\text{GeV}/c)^2$. The data were obtained by performing a coincidence between the SLAC 1.6 GeV/ c spectrometer and a lucite shower counter. The scattering appears diffractive out to high t -values, but the cross sections seem not to be in good agreement with the prediction of a strict Vector Meson Dominance Model.

(Submitted to Phys. Rev. Letters.)

(Also submitted to the International Conference on High Energy Physics, 26 August - 4 September 1970, Kiev, USSR.)

*Work supported by the U. S. Atomic Energy Commission.

Compton scattering is interesting as one of the basic reactions involving photons and protons. It is expected to be predominantly diffractive at low t -values but possibly to become nondiffractive at larger momentum transfers. Previous to this experiment, data were available only up to incident photon energies of 1.5 GeV.¹ We report here our measurement of the differential cross sections for incident photon energies between 5 GeV and 17 GeV and for the four momentum transfer squared between $-0.06 (\text{GeV}/c)^2$ and $-1.1 (\text{GeV}/c)^2$.

The results of this experiment are particularly useful within the context of the Vector Meson Dominance Model.² In this model the Compton cross section is directly related to the known cross sections³ for photoproduction of vector mesons. Knowledge of the Compton cross section at high energies therefore makes possible a direct test of the model.

A comparison between the total photoabsorption cross section σ_T and the forward Compton cross section at $t=0$ is also important. Such a comparison serves as a check on the forward dispersion relations.⁴ These relations have been well established in elastic πN scattering. However, in the case of photons additional terms,⁵ which are absent in πN scattering, may be added to the real part of the diffractive amplitude. The limits⁶ on such terms, previous to this experiment, were rather poor.

The layout of the experiment is shown in Fig. 1. A well collimated photon beam passed through a hydrogen target and a helium duct, and stopped in a Secondary Emission Quantameter (SEQ). In addition to the quantameter, which was the primary beam monitor, the intensity was monitored by a Cerenkov cell located in front of the target. Both of these instruments were calibrated periodically with a calorimeter. An electron beam was frequently used in the experiment to check apertures and to calibrate the equipment. The intensity of this electron beam was monitored by a toroid in front of the target and by the SEQ.

For large t -values ($|t| \geq .4 \text{ (GeV/c)}^2$) a conventional liquid target cell was used. For small t -values we used a high pressure gas target,⁷ cooled to 34° K with a commercial refrigerator unit. The density of the hydrogen in the gas target was $.01 \text{ gm/cm}^3$. The target was connected directly to the spectrometer vacuum and the protons left the hydrogen through a $.025 \text{ cm}$ thick mylar window. This reduced the material the protons passed through before reaching the exit window of the spectrometer to less than $.002$ of a radiation length.

The scattered photon passed through a helium duct and a sweeping magnet, and was detected in a shower counter. The arrangement of the shower counter is shown in detail in the insert of Fig. 1. The shower counter proper was a conventional lead-lucite sandwich counter 13 radiation lengths thick. The counter was placed inside a well shielded cave, which could be moved remotely in angle and in height. The aperture of the counter was defined by remotely movable lead slits in front of the counter. To reduce the pileup from low energy photons, 3 radiation lengths of carbon were placed just in front of the counter.

The momentum and angle of the proton were measured by the SLAC 1.6 GeV/c spectrometer. The counter system in the spectrometer is shown in detail in the insert in Fig. 1 and consists mainly of a range telescope and a missing mass hodoscope. The first two backing counters, located in front of the hodoscope, are each only $.08 \text{ cm}$ thick. A coincidence between these and the missing mass hodoscope was sufficient to define a clean proton signal for $|t|$ less than $.2 \text{ (GeV/c)}^2$. For $|t|$ larger than $.4 \text{ (GeV/c)}^2$ a threshold lucite Cerenkov counter was used to veto pions. In addition to the missing mass hodoscope we also had a momentum hodoscope made of $.08 \text{ cm}$ thick scintillator. The momentum hodoscope in effect reduced the spread in flight times through the spectrometer, so that shorter resolving times for the coincidence between the proton telescope and the shower counter could be used.

The recoil proton and the incoming photon defined the plane of elastic scattering. Photoproduced π^0 mesons, which were the main source of background in the experiment, decay into two photons with a typical half-opening angle of (m_π/E_π) . However, since the solid angle of the shower counter (matched to the spectrometer acceptance) was small compared with this decay cone, the π^0 contamination was strongly suppressed. The remaining π^0 contribution, including accidental counts, was measured directly by moving the shower counter out of the Compton plane. The main event selection was therefore made by the spectrometer, and the shower counter simply provided an additional kinematic constraint. This constraint was largely geometric in nature and not strongly dependent on the energy resolution of the counter. This was important, since the high instantaneous rates at SLAC make a good energy measurement of the photon very difficult without severely limiting the data taking rate.

The acceptance of the system was well defined. The spectrometer determined the t -value, the t -acceptance and the effective target length. The acceptance in photon energy $\Delta k/k$ and the vertical angle $\Delta\phi$ were determined by the horizontal and vertical slits in front of the shower counter. During the experiment Δt varied from $.007 \text{ (GeV/c)}^2$ at the lowest t -values to $.09 \text{ (GeV/c)}^2$ at 1.1 (GeV/c)^2 , $\Delta k/k$ was typically 10%, and $\Delta\phi$ varied from 0.7 mrad to 7 mrad depending upon the kinematics. $\Delta\phi$ was always kept small compared to (m_π/E_π) .

As a check on the acceptance as well as the overall alignment of the system, cross sections for elastic e - p scattering were measured detecting the recoil proton in coincidence with the scattered electron. Elastic e - p scattering has the same kinematics as Compton scattering at high energy. The response of the shower counter to electron and photon beams is very nearly the same and the cross sections are well known for the momentum transfers of our experiment.

The data was corrected for counter efficiencies, losses due to multiple scattering, and for radiative effects according to Meister and Yennie.⁸ The resultant cross sections at all energies are in agreement with earlier measurements⁹ indicating that the acceptance of the system is well understood.

Figure 2a shows a γ -p coincidence peak for an incident photon energy of 12 GeV and $-t = .5 (\text{GeV}/c)^2$. Plotted is the coincidence yield versus missing mass for the shower counter in and out of the Compton plane. The width of the peak is mainly due to multiple scattering of the recoil proton. The contribution from π^0 photoproduction measured with the shower counter out of the Compton plane is small, as expected, although the π^0 cross section is comparable to the Compton cross section for this t -value and energy. Figure 2b shows the result of subtracting the out-of-plane yield from the in-plane yield. The resultant curve is our experimental Compton yield. The yield goes to zero on both sides of the peak indicating that the accidental counts are properly subtracted and background from many-body processes is negligible. Since the π^0 detection efficiency (C) in the Compton plane is slightly greater than the π^0 detection efficiency (C') out-of-the plane, a small residual π^0 signal still remains in the Compton peak. This residual π^0 signal is given by $(1-C'/C)$ times the measured π^0 rate, and is generally small. For the yields of Fig. 2b it is less than a 1% correction. The largest correction was at 18 GeV and $t = -1.1 (\text{GeV}/c)^2$ where it amounted to about 8%. Corrections for these residual π^0 signals were determined by computing the ratio (C'/C) . In general this ratio was kept approximately equal to 0.9. We have checked the computation by evaluating the π^0 cross sections using the computed value of C' and the measured π^0 yields. The π^0 cross sections determined in this way are in agreement with our single arm measurements.¹⁰

The Compton data were corrected for counter efficiencies, loss from pair production of the scattered photon before the sweeping magnet, loss of incident photons before the SEQ, and the change in the Δt acceptance of the spectrometer due to energy loss of the proton in the target. The total corrections were typically about 30% and were largely determined experimentally. The total uncertainty introduced by these corrections is conservatively assumed to be 20% of the correction.

The corrected cross sections are listed in Table I and plotted versus t in Fig. 3 for effective photon energies of 5.5, 8.5, 11.5, and 17 GeV. The data include all the errors except an overall normalization error of about 5%.

The solid lines through the data points are the results of a least squares fit to the data of the form Ae^{Bt+Ct^2} . The values of the parameters from this fit are listed in Table II. In the range of $|t| \leq .6$ (GeV/c)² we obtain a good fit to the data at all energies using a single exponential with a slope of approximately 6 (GeV/c)⁻². However, at 17 GeV we cannot fit the data in the whole t range with a single exponential.

The forward amplitude in Compton scattering is given by:

$$f = \left(\epsilon_2^* \cdot \epsilon_1 \right) f_1 + i \underline{\sigma} \cdot \left(\epsilon_2^* \times \epsilon_1 \right) f_2$$

Here, ϵ_1 , ϵ_2 are the polarization vectors of the photon before and after the scattering and $\underline{\sigma}$ the Pauli spin matrix of the recoil proton. Using the optical theorem, $\text{Im} f_1 = (k/4\pi) \sigma_T$, the forward cross section $(d\sigma/dt)_{t=0}(k)$ can be written as

$$\left(\frac{d\sigma}{dt} \right)_{t=0}(k) = \frac{\sigma_T^2}{16\pi} + \pi/k^2 |\text{Re } f_1|^2 + \pi/k^2 |f_2|^2$$

This relation was evaluated, neglecting f_2 and using values for σ_T as measured by Caldwell et al.¹¹ and the real part of f_1 as computed by Damashek and Gilman.⁴

The results are shown as the squares in Fig. 3. The $t=0$ intercepts of the fits to our data are in fair agreement with these optical points, although on the average they are somewhat low. The results are therefore consistent with f_2 equal to zero. It is possible, to first order in α , to add terms of the type $\lambda_1 k^2$ to the real part of f_1 without disturbing the unitary limit or the Thompson limit as k approaches zero.⁵ To set a limit on the term $\lambda_1 k^2$ we assume that this term contributes at the most $.05 \mu\text{b}/\text{GeV}^2$ to the cross section at 17 GeV. The limit corresponds to keeping the optical point fixed and increasing our measured forward cross section by 3 standard deviations. The corresponding limit of λ_1 is $7.4 \times 10^{-5} \text{ fm}/\text{GeV}^2$. This value of λ_1 corresponds to a change in slope of the Compton cross section near π^0 threshold⁵ of about .04%.

The relationship between the amplitude $f_{\gamma\gamma}$ for Compton scattering and the amplitude $f_{\gamma V}^{\text{tr}}$ for the photoproduction of a transversely polarized vector meson V is given by Vector Meson Dominance Model as:

$$f_{\gamma\gamma} = \sum_{\rho, \omega, \phi} g_{\gamma V} \cdot f_{\gamma V}^{\text{tr}}$$

Here $g_{\gamma V}$ is the direct photon vector meson coupling constant. The numerical values were taken from the recent determinations by the Orsay storage ring group.¹² The amplitudes $f_{\gamma\rho}^{\text{tr}}$ and $f_{\gamma\phi}^{\text{tr}}$ were taken from our earlier measurements of ρ and ϕ photoproduction,¹³ assuming the whole amplitude to be transverse. For ρ -photoproduction this has been shown to be true for $|t|$ -values less than $.4 (\text{GeV}/c)^2$.¹⁴ In general this assumption provides us with an upper limit on the Compton cross section. The amplitude $f_{\gamma\omega}^{\text{tr}}$ was set equal to $1/3 f_{\gamma\rho}^{\text{tr}}$, but the fits do not depend strongly upon this assumption. The results are shown in Fig. 3 as the dashed lines. They are systematically lower and the slope is steeper than our data. Using the values of $f_{\gamma V}^2$ as measured¹⁵ on the photon mass shell tend to increase the discrepancy even further. This experiment then

demonstrates that the photon is not completely described by the three vector mesons but that the photon also couples strongly to other states. This breakdown of the strict Vector Meson Dominance Model has also shown up in the differences between $g_{\gamma\rho}^2$ as determined by the total cross section measurements on one hand and by ρ -photoproduction experiments on the other.

J. Grant, E. Cheatham, J. Escalera, and J. Schroeder gave us invaluable support with the setup and the preparations for the experiment. We wish to acknowledge the help we received from the operations and support crew at Stanford Linear Accelerator Center, and especially we wish to thank D. Coward, R. Eisele, R. Filippi, A. Golde, G. Nabi, and E. Taylor.

REFERENCES

1. R. F. Stiening et al., Phys. Rev. Letters 10, 536 (1963);
M. Deutsch et al., Proceedings of the 3rd International Symposium on Electron and Photon Interactions at High Energies, Stanford Linear Accelerator Center, 1967 (Clearing House of Federal Scientific and Technical Information, Washington, D.C., 1968); D. R. Rust et al., Phys. Rev. Letters 15, 938 (1965); E. Eisenhandler et al., Phys. Letters 24B, 347 (1967).
2. J. J. Sakurai, Proceedings of the 4th International Symposium on Electron and Photon Interactions at High Energies, Daresbury Nuclear Physics Laboratory, Liverpool (1969).
3. A. Silverman, Proceedings of the 4th International Symposium on Electron and photon Interactions at High Energies, Daresbury Nuclear Physics Laboratory, Liverpool (1969).
4. M. Gell-Mann, M. L. Goldberger and W. Thirring, Phys. Rev. 95, 1612 (1954); M. Damashek and F. J. Gilman, Phys. Rev. D1, 1319 (1970).

5. S. D. Drell, Proceedings of the 3rd International Symposium on Electron and Photon Interactions at High Energies, Stanford Linear Accelerator Center, 1967 (Clearing House of Federal Scientific and Technical Information, Washington, D.C., 1968).
6. J. K. Walker, Phys. Rev. Letters 21, 1618 (1968).
7. J. Grant and B. H. Wiik (to be published).
8. N. Meister and D. Yennie, Phys. Rev. 130, 1210 (1963).
9. T. Janssens et al., Phys. Rev. 142, 922 (1966).
10. R. L. Anderson et al., (to be published in Phys. Rev. Letters).
11. D. O. Caldwell et al., (to be published in Phys. Rev. Letters).
12. J. Perez-y-Jorba, Proceedings of the 4th International Symposium on Electron and Photon Interactions at High Energies, Daresbury Nuclear Physics Laboratory, Liverpool (1969).
13. R. L. Anderson et al., Phys. Rev. D1, 27 (1970).
14. J. Ballam et al., Phys. Rev. Letters 24, 960 (1970).
15. J. G. Asbury et al., Phys. Rev. Letters 20, 227 (1968); G. McClellan et al., Phys. Rev. Letters 22, 377 (1969); F. Bulos et al., Phys. Rev. Letters 22, 490 (1969); R. L. Anderson et al., (to be published in Phys. Rev. Letters).

TABLE I

$d\sigma/dt$ in $\mu\text{barns}/(\text{GeV}/c)^2$

t	5.5 GeV	8.5 GeV	11.5 GeV	17 GeV
.06			.441 \pm .063	
.1	.424 \pm .044	.309 \pm .039	.334 \pm .028	.302 \pm .023
.15	.355 \pm .030			
.2	.225 \pm .017	.179 \pm .015	.171 \pm .011	.143 \pm .0088
.3	.141 \pm .015	.114 \pm .011	.0952 \pm .0090	.0850 \pm .0070
.4	.0648 \pm .0056	.0538 \pm .0046	.0499 \pm .0041	.0480 \pm .0046
.5	.0410 \pm .0033	.0343 \pm .0027	.0312 \pm .0026	.0266 \pm .0024
.6	.0230 \pm .0041	.0191 \pm .0018	.0165 \pm .0015	.0153 \pm .0013
.7		.0105 \pm .0011	.0090 \pm .00098	.0076 \pm .0016
.8		.00853 \pm .0015	.0055 \pm .00070	.00570 \pm .00063
.9				.00326 \pm .00037
1.1				.00138 \pm .00022

TABLE II

Fits to Data of Form $d\sigma/dt = Ae^{Bt} + Ct^2$

	5.5 GeV	8.5 GeV	11.5 GeV	17 GeV
A $\mu\text{b}/(\text{GeV}/c)^2$.88 \pm .15	.6 \pm .1	.63 \pm .06	.55 \pm .05
B $(\text{GeV}/c)^{-2}$	6.9 \pm 1.3	6.2 \pm 0.8	6.5 \pm 0.6	6.6 \pm 0.4
C $(\text{GeV}/c)^{-4}$	1.3 \pm 1.9	.7 \pm .9	.8 \pm .7	1.1 \pm .4
χ^2 / Degree of Freedom	0.93	0.94	0.25	0.41

FIGURE CAPTIONS

1. Experimental arrangement.
2. Compton yields: (a) Yield curves with shower counter in the Compton plane ($\gamma + \pi^0$) and out of the Compton plane (π^0); (b) Difference between the two curves in (a).
3. Compton cross sections $d\sigma/dt$ in $\mu\text{b}/(\text{GeV}/c)^2$ are plotted versus t for incident photon energies of 5.5, 8.5, 11.5, and 17 GeV. The solid lines are the result of a least square fit of the form Ae^{Bt+Ct^2} to the data. The dashed curves are the predictions from the V.D.M. as explained in the text. The optical points shown include the real part as computed by Damashek and Gilman.

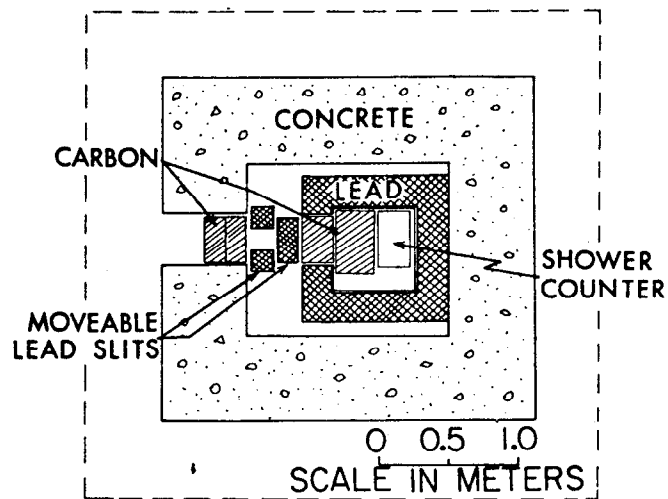
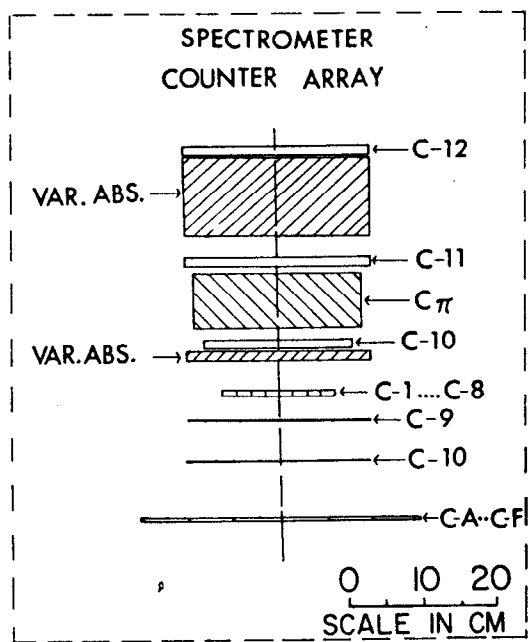
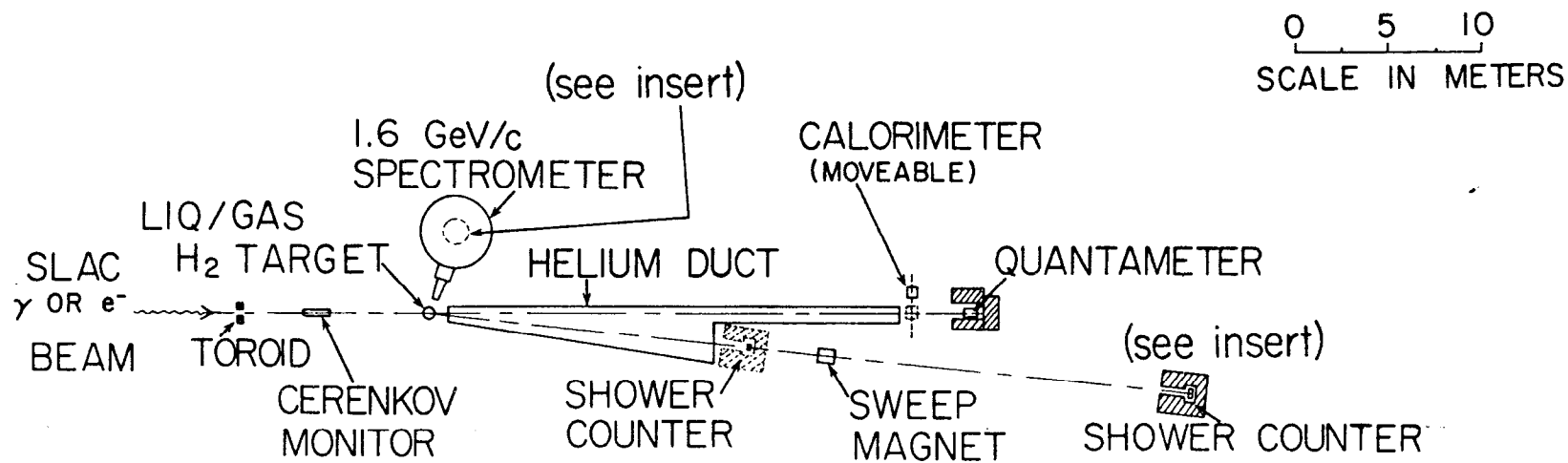


Fig. 1

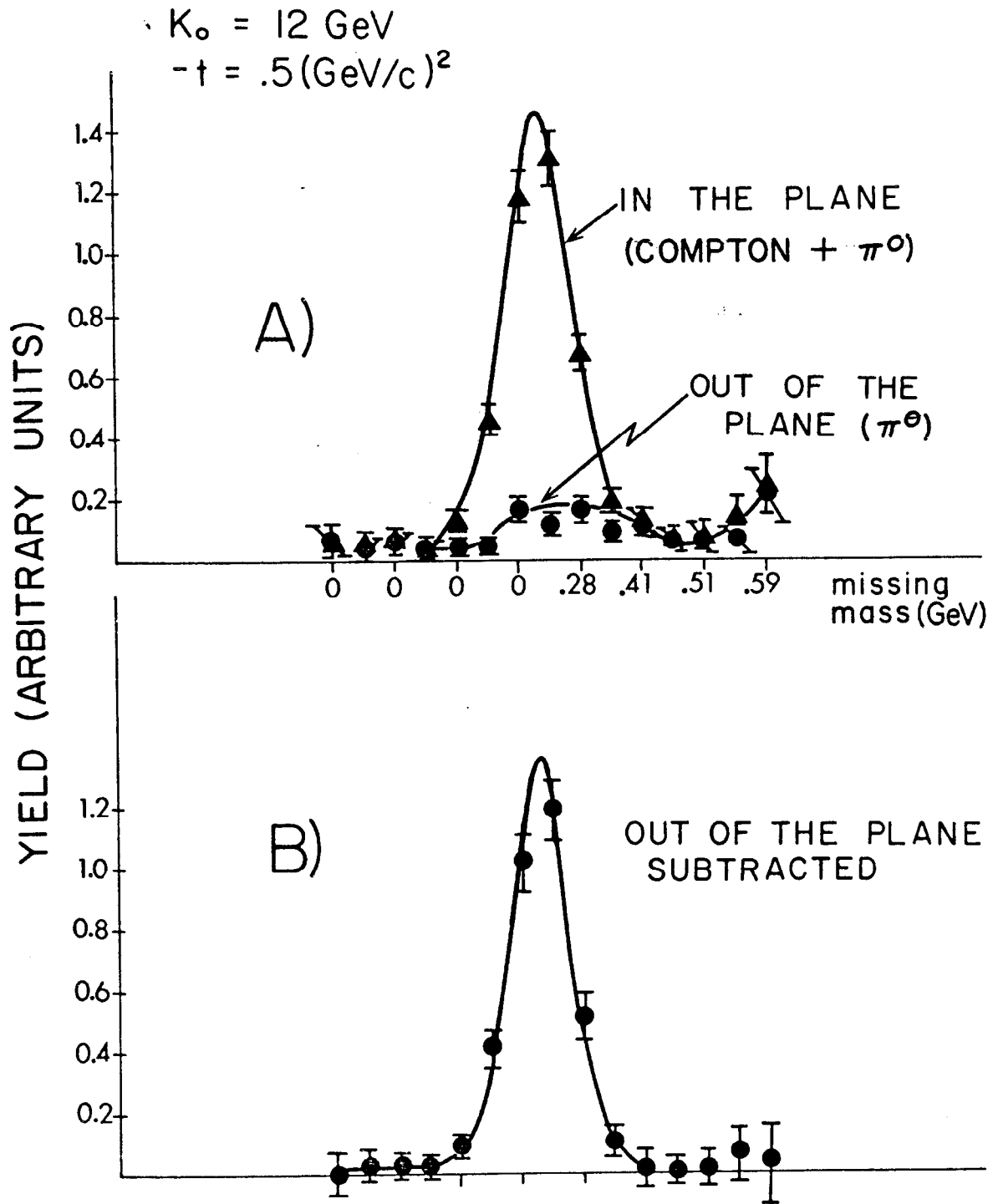


Fig. 2

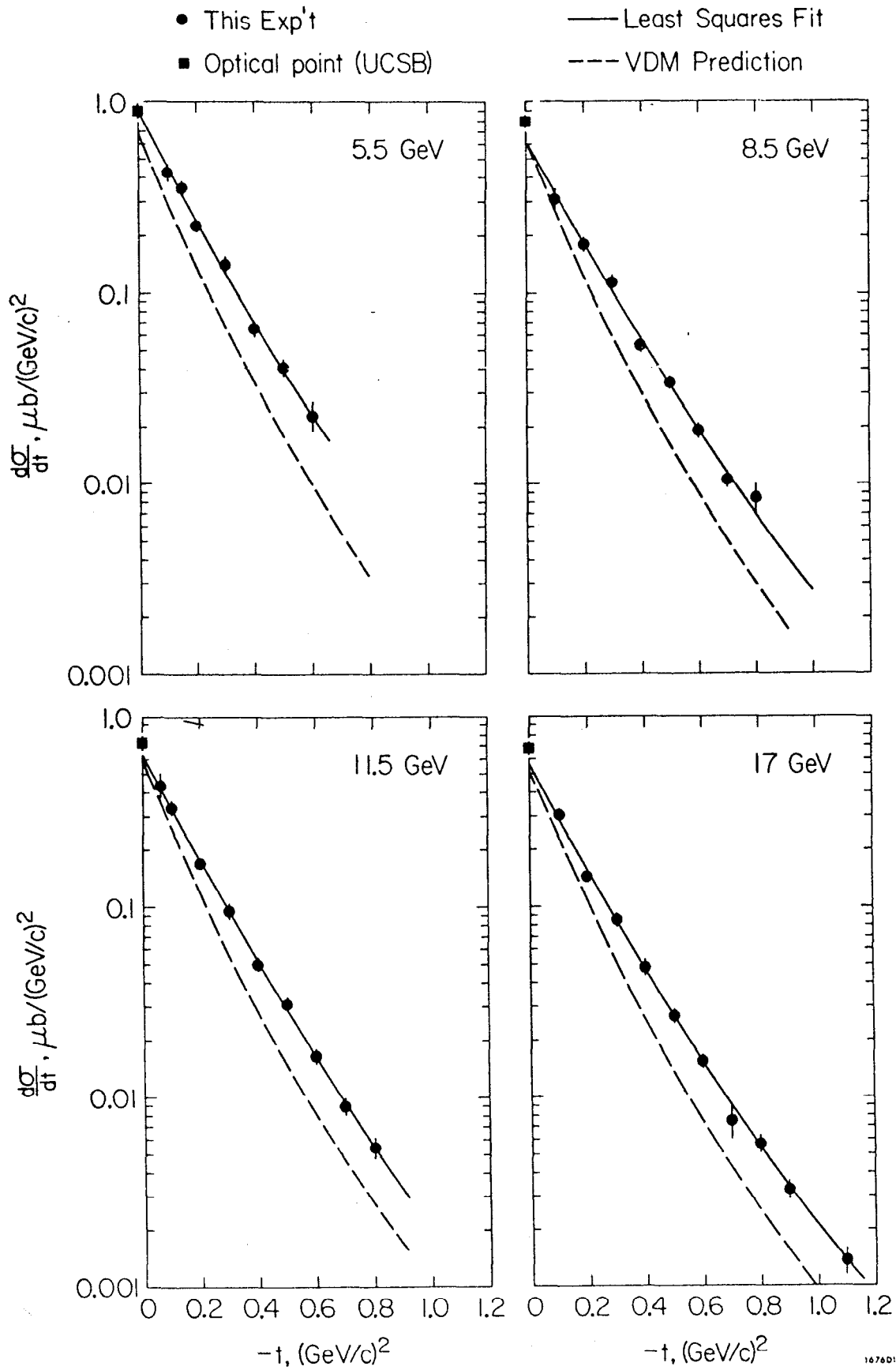


Fig. 3